This article was downloaded by: [Renmin University of China]
On: 13 October 2013, At: 10:48
Publisher: Taylor & Francis
Informa Ltd Registered in England and Wales Registered Number: 1072954 Registered office: Mortimer House, 37-41 Mortimer Street, London W1T 3JH, UK

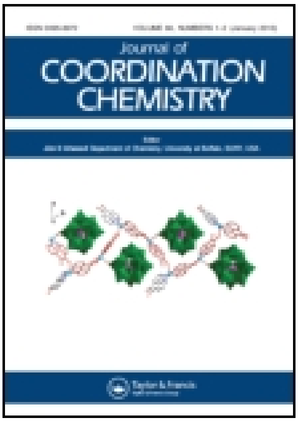

Journal of Coordination Chemistry
Publication details, including instructions for authors and subscription information:
http://www.tandfonline.com/loi/gcoo20

# Zinc coordination polymers with rigid dicarboxylates and semirigid 3,5-bis(imidazole-1-yl) pyridine: syntheses, structural topologies, and luminescent properties

Jiakun Xu [a] , Xiaochun Sun [b] , Caixia Ju [a c] , Jun Sheng [a] , Fang Wang [a] & Mi Sun [a]

[a] Yellow Sea Fisheries Research Institute , Chinese Academy of Fishery Sciences , Qingdao , China

[b] National Oceanographic Center , Qingdao , China

[c] College of Food Science and Technology , Shanghai Ocean University , Shanghai , China

Accepted author version posted online: 28 May 2013.Published online: 26 Jun 2013.

To cite this article: Jiakun Xu , Xiaochun Sun , Caixia Ju , Jun Sheng , Fang Wang & Mi Sun (2013) Zinc coordination polymers with rigid dicarboxylates and semirigid 3,5-bis(imidazole-1-yl) pyridine: syntheses, structural topologies, and luminescent properties, Journal of Coordination Chemistry, 66:14, 2541-2548, DOI: 10.1080/00958972.2013.809423

To link to this article: http://dx.doi.org/10.1080/00958972.2013.809423

PLEASE SCROLL DOWN FOR ARTICLE

Taylor & Francis makes every effort to ensure the accuracy of all the information (the “Content”) contained in the publications on our platform. However, Taylor & Francis, our agents, and our licensors make no representations or warranties whatsoever as to the accuracy, completeness, or suitability for any purpose of the Content. Any opinions and views expressed in this publication are the opinions and views of the authors, and are not the views of or endorsed by Taylor & Francis. The accuracy of the Content should not be relied upon and should be independently verified with primary sources of information. Taylor and Francis shall not be liable for any losses, actions, claims, proceedings, demands, costs, expenses, damages, and other liabilities whatsoever or howsoever caused arising directly or indirectly in connection with, in relation to or arising out of the use of the Content.

*Journal of Coordination Chemistry*, 2013
Vol. 66, No. 14, 2541–2548, http://dx.doi.org/10.1080/00958972.2013.809423

Taylor & Francis
Taylor & Francis Group

# Zinc coordination polymers with rigid dicarboxylates and semirigid 3,5-bis(imidazole-1-yl) pyridine: syntheses, structural topologies, and luminescent properties

JIAKUN XU*†, XIAOCHUN SUN‡, CAIXIA JU†§, JUN SHENG†, FANG WANG† and MI SUN*†

†Yellow Sea Fisheries Research Institute, Chinese Academy of Fishery Sciences, Qingdao, China
‡National Oceanographic Center, Qingdao, China
§College of Food Science and Technology, Shanghai Ocean University, Shanghai, China

(*Received 14 October 2012; in final form 18 April 2013*)

Two metal coordination polymers, $\{[Zn(bpdc)(bip)]\cdot 2H_2O\}_n$ (**1**) and [Zn(tdc)(bip)] (**2**) [$H_2$bpdc = biphenyl-4,4'-dicarboxylate, $H_2$tdc = thiophene-2,5-dicarboxylate, bip = 3,5-bis(imidazole-1-yl)pyridine], have been synthesized and characterized by IR, elemental analysis, XRD, and X-ray single-crystal diffraction. In **1**, bpdc and bip link Zn(II) ions into a corrugated 2D layer. The corrugated 2D layers polycatenate each other, yielding a 2D→3D polycatenation net. In **2**, dinuclear Zn(II) units are formed by bip and further connected by tdc to construct a 2D 3-connected framework. The luminescent properties of **1** and **2** are investigated in the solid state at room temperature.

*Keywords*: Zinc(II) coordination polymers; Crystal structure; Luminescence

## 1. Introduction

Interest in coordination polymers (CPs) or metal-organic frameworks stems from potential applications in storage [1–3], luminescence [4, 5], drug delivery [6], magnetism [7], catalysis [8, 9], separation [10] and sensors [11], and from fascinating architectures and intriguing topologies [12]. Various ligands are of importance for structural diversity of CPs and provide new insights into the relationships between the structure and the corresponding function. Multidentate rigid ligands, such as benzenetricarboxylic acid as well as its deprotonated anions ($H_3BTC$, $H_2BTC^-$, $HBTC^{2-}$, and $BTC^{3-}$) [13, 14], and 4,4′,4″-benzene-1,3,5-triyl-tribenzoic acid (including deprotonated anions: $H_3BTB$, $H_2BTB^-$, $HBTB^{2-}$, and $BTB^{3-}$) [15, 16], have prepared a variety of CPs. Flexible ligands have been utilized for the construction of coordination networks with special properties and structures [17–19], contributing insight into details of self-assembly processes. However, the possibility of diverse ligand conformations makes it difficult to control the architectures of CPs based on flexible ligands, and the structural characterizations also appear to be more challenging. In

---

*Corresponding authors. Email addresses: xujk@ysfri.ac.cn (Jiakun Xu); hhsunmi@yeah.net (Mi Sun)

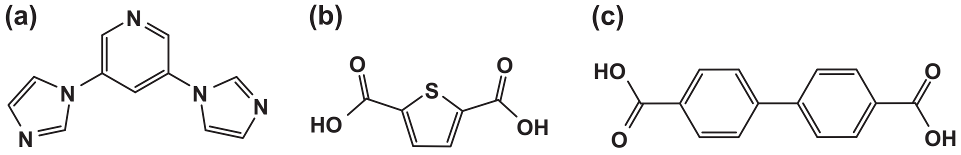

Scheme 1. Chemical structures of the ligands: (a) 3,5-bis(imidazole-1-yl)pyridine, (b) thiophene-2,5-dicarboxylic acid, and (c) biphenyl-4,4'-dicarboxylic acid.

contrast, semirigid ligands have received attention owing to slight conformational changes during assembly [20–24], which avoids problems associated with flexible ligands. Zinc is promising for construction of CPs and networks due to the spherical $d^{10}$ configuration [25], accommodating various polymer architectures [26–32].

In this context, the semirigid organic linker (3,5-bis(imidazole-1-yl)pyridine, 3,5-bip) provided a cooperative coordination with the rigid dicarboxylates ($H_2$bpdc = biphenyl-4,4′-dicarboxylate and $H_2$tdc = thiophene-2,5-dicarboxylate) (scheme 1) to meet the coordination geometries of metal ions in the assembly process. We herein report two Zn(II) CPs obtained from 3,5-bip and $H_2$bpdc or $H_2$tdc.

## 2. Experimental

### 2.1. *Materials and physical measurements*

All reagents and solvents were commercially available and used as received. Elemental analysis was carried out on a Carlo Erba 1106 full-automatic trace organic elemental analyzer. FTIR spectra were recorded with a Bruker Tensor-27 FTIR spectrometer as a dry KBr pellet from 400 to 4000 $cm^{-1}$. Solid-state fluorescence spectra were recorded on a

Table 1. Crystallographic data and structure refinement summary for **1** and **2**.

| | | |
|---|---|---|
| Empirical formula | $C_{25}H_{21}ZnN_5O_6$ | $C_{17}H_{11}ZnSN_5O_4$ |
| Formula weight | 522.84 | 446.74 |
| Crystal system | Orthorhombic | Monoclinic |
| Space group | $P2_12_12_1$ | $P2_1/n$ |
| Unit cell dimensions | $a = 8.067(5)$ Å | $a = 8.813(5)$ Å |
| | $b = 11.694(5)$ Å | $b = 20.004(5)$ Å |
| | $c = 25.916(5)$ Å | $c = 9.686(5)$ Å |
| | $\beta = 90°$ | $\beta = 95.740(5)°$ |
| Volume (Å$^3$) | 2444.8(19) | 1699.0(14) |
| $Z$ | 4 | 4 |
| Calculated density (mg/m$^3$) | 1.502 | 1.746 |
| Independent reflections ($I > 2\sigma(I)$) | 5063 | 3409 |
| $F$ (000) | 1136 | 904 |
| $\theta$ range for data collection | 1.57–27.53 | 2.04–27.56 |
| Limiting indices | $-8 \leqslant h \leqslant 10$ | $-11 \leqslant h \leqslant 11$ |
| | $-14 \leqslant k \leqslant 14$ | $-13 \leqslant k \leqslant 26$ |
| | $-33 \leqslant l \leqslant 32$ | $-12 \leqslant l \leqslant 12$ |
| *Goodness-of-fit on* $F^2$ | | |
| $R_1{}^a$, $wR_2{}^b$ [$I > 2\sigma(I)$] | $R_1 = 0.0291$, $wR_2 = 0.0332$ | $R_1 = 0.0263$, $wR_2 = 0.0688$ |
| $R_1{}^a$, $wR_2{}^b$ (all data) | $R_1 = 0.0724$, $wR_2 = 0.0741$ | $R_1 = 0.0313$, $wR_2 = 0.0711$ |
| Largest diff. peak and hole (e/Å$^3$) | 0.338 and −0.208 | 0.338 and −0.256 |

$^aR = \sum(||F_0| - |F_C||)/\sum|F_0|$.
$^bwR = [\sum w(|F_0|^2 - |F_C|^2)^2/\sum w(F_0{}^2)]^{1/2}$.

Table 2. Selected bond lengths (Å) and angles (°) for **1** and **2**.

| | | | |
|---|---|---|---|
| Compound **1** | | | |
| Zn(1)–N(1) | 1.990(2) | Zn(1)–O(1) | 1.952(2) |
| Zn(1)–N(5) | 2.042(2) | Zn(1)–O(3) | 1.927(2) |
| O(3)–Zn(1)–N(1) | 124.12(7) | O(1)–Zn(1)–N5 | 96.64(7) |
| O(1)–Zn(1)–N(1) | 114.10(8) | N(1)–Zn(1)–N5 | 106.04(8) |
| O(3)–Zn(1)–N5 | 98.16(8) | | |
| Compound **2** | | | |
| Zn(1)–O(4)$^{a}$ | 1.938(2) | Zn(1)–N(4)$^{b}$ | 2.001(2) |
| Zn(1)–O(1) | 1.966(1) | Zn(1)–N(1) | 2.007(2) |
| O(4)$^{a}$–Zn(1)–O(1) | 119.54(6) | O(4)$^{a}$–Zn(1)–N(1) | 102.37(7) |
| O(4)$^{a}$–Zn(1)–N(4)$^{b}$ | 110.22(6) | O(1)–Zn(1)–N(1) | 102.16(6) |
| O(1)–Zn(1)–N(4)$^{b}$ | 109.04(7) | N4$^{b}$–Zn(1)–N(1) | 113.19(7) |

Symmetry code for **2**: $^{a}x-1/2,\ -y+3/2,\ z-1/2$; $^{b}-x+1,\ -y+2,\ -z+1$.

Hitachi F-4600 equipped with a xenon lamp and a quartz carrier at room temperature. X-ray powder diffraction (XRPD) measurements were performed on a Bruker D8 diffractometer operated at 40 kV and 40 mA using Cu-K$\alpha$ radiation ($\lambda = 0.15418$ nm).

## 2.2. *Syntheses*

**2.2.1. {[Zn(bpdc)(bip)]·2H$_2$O}$_n$ (1).** A mixture of Zn(NO$_3$)$_2$·6H$_2$O (0.297 g, 1 mmol), H$_2$bpdc (0.242 g, 1 mmol), bip (0.211 g, 1 mmol), NaOH (0.08 g, 2 mmol), and deionized water (18 mL) was sealed in a 25 mL Teflon-lined stainless steel vessel and heated at 160 °C for 96 h. After cooling to room temperature, colorless block crystals were obtained and washed with alcohol several times (Yield: 32% based on Zn). Elemental Anal. Calcd (%) for $C_{25}H_{21}ZnN_5O_6$: C, 54.31; H, 3.83; N, 12.67. Found: C, 54.34; H, 3.81; N, 12.68. IR: 3214 br, 1628 s, 1417 m, 1328 m, 1264 m, 1142 m, 975 m, 867 m, 737 m.

**2.2.2. [Zn(tdc)(bip)] (2).** Compound **2** was obtained by hydrothermal procedure as for preparation of **1** only using H$_2$tdc (0.172 g, 0.1 mmol) instead of H$_2$bpdc. Colorless block crystals of **2** were collected in 40% yield based on Zn after washing by ethanol several times. Elemental Anal. Calcd (%) for $C_{17}H_{11}ZnSN_5O_4$: C, 45.70; H, 2.48; N, 15.68. Found: C, 45.68; H, 2.49; N, 15.69. IR: 1646 s, 1434 s, 1355 m, 1236 m, 1101 m, 1038 m, 924 m, 857 w, 766 m.

## 2.3. *Single-crystal structure determination*

Diffraction intensity data of the single crystals were collected on a Bruker SMART APEX II CCD diffractometer equipped with graphite monochromated Mo-*K*$\alpha$ radiation ($\lambda = 0.71073$ Å) by using a $\omega$-scan mode. Empirical absorption correction was applied using SADABS [33]. All the structures were solved by direct methods and refined by full-matrix least-squares on $F^2$ using SHEXL 97 [34]. All non-hydrogen atoms were refined anisotropically. Hydrogens were located by geometric calculations, and their positions and thermal parameters were fixed during the structure refinement. Crystallographic data are summarized in table 1. Relevant bond lengths and angles are listed in table 2.

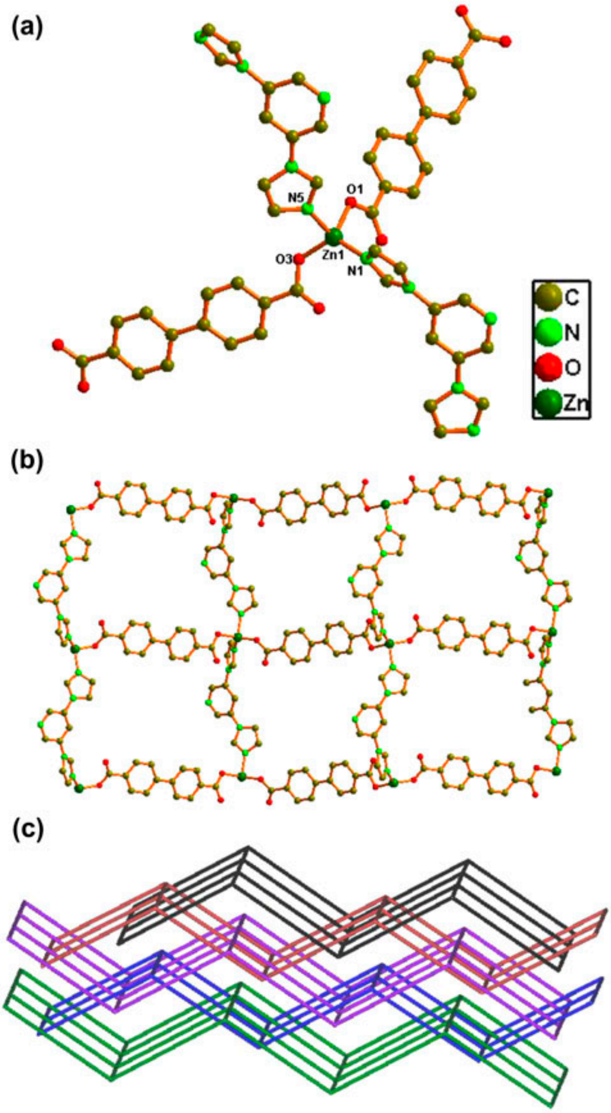

Figure 1. (a) The coordination environment for Zn(II) in **1**; (b) the 2D layer formed by pbdc anions and 3,5-bip ligand; and (c) the 2D→3D polycantenated structure in **1**.

## 3. Results and discussion

### 3.1. *Description of crystal structures*

**3.1.1. $\{[Zn(bpdc)(bip)]\cdot 2H_2O\}_n$ (1).** The fundamental building unit of **1** consists of one zinc(II), one pbdc, and one 2,6-bip (figure 1(a)). The Zn(II) center is coordinated by two carboxylate oxygens from the different pbdc ligands [Zn(1)–O(1) = 1.952(2) and Zn(1)–O(3) = 1.927(2) Å] and two nitrogens from two 2,6-bip ligands [Zn(1)–N(1) = 1.990(2) and Zn(1)–N(5) = 2.042(2) Å] in a distorted tetrahedral environment. The Zn(II) ions are linked by pbdc anions and 2,6-bip to form deeply corrugated 2D (4, 4) sheets (figure 1(b)). Each

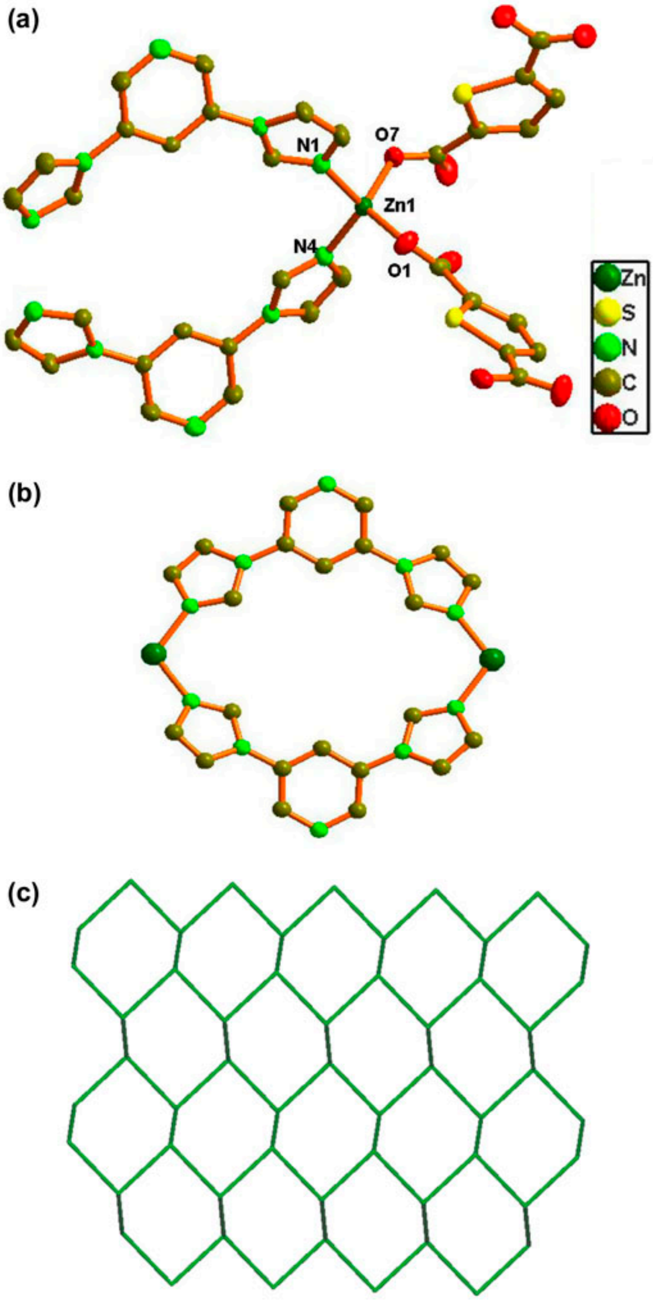

Figure 2. (a) The coordination environment for Zn(II) in **2**; (b) the dinuclear Zn(II) unit formed by 3,5-bip; and (c) the 2D layer structure for **2**.

four-membered ring is constructed by four Zn(II) ions, two pbdc, and two 3,5-bip ligands. A nanosized cavity with approximate dimension of 15.1 × 11.7 Å is observed (based on distances of Zn…Zn). The open space within each sheet leads to formation of catenation

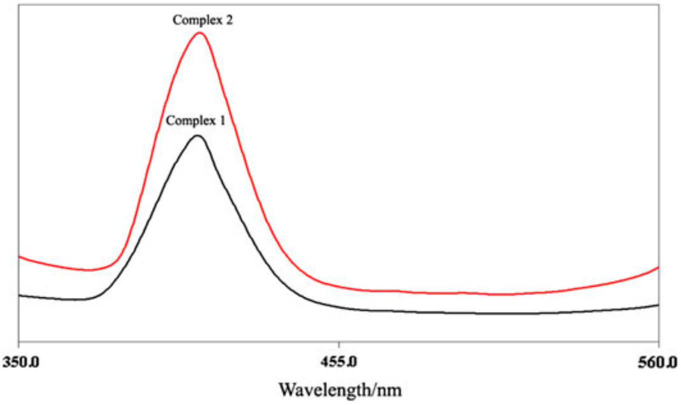

Figure 3. Fluorescent emission spectra for **1** and **2** in the solid state at room temperature.

between adjacent sheets that are parallel and crystallographically equivalent. This results in an infinite parallel polycatenation of the 4-connected layer. Each layer is penetrated by two others (one above and one below) which have parallel but not coincident mean planes, leading to an overall 3D entanglement (figure 1(c)).

**3.1.2. [Zn(tdc)(bip)] (2).** Single-crystal X-ray analysis revealed that the unsymmetrical unit of **2** is constructed by one zinc(II), one tdc, and 3,5-bip. Zn(II) is four-coordinate and exhibits a distorted tetrahedral geometry, surrounded by two carboxylate oxygens [Zn(1)–O(1) = 1.966(1) and Zn(1)–O(4) = 1.938(2) Å] and two nitrogens [Zn(1)–N(1) = 2.007(2) and Zn(1)–N(4) = 2.001(2) Å] (figure 2(a)). The 2,6-bip ligands link Zn(II) to form a dinuclear Zn(II) unit [the distance of Zn…Zn is 10.155 Å] (figure 2(b)). If the dinuclear Zn(II) can be viewed as a node, the 2D network can be simplified as a 3-connected topological net with the symbol of ($6^3$) (figure 2(c)).

### 3.2. *XRPD analysis and luminescent properties*

To confirm the purity of the samples, **1** and **2** are measured by XRPD. Experimental and simulated XRPD patterns of **1** and **2** are shown in Supplementary material. All peaks in the measured curves approximately match the simulated curves generated from single-crystal diffraction data, which clearly confirms the phase purity of the as-synthesized products.

The fluorescence emission spectra of **1** and **2** were measured in the solid state at room temperature (figure 3). Intense luminescence emission bands of **1** and **2** are observed at 408 nm ($\lambda_{ex} = 280$ nm) and 409 nm ($\lambda_{ex} = 280$ nm), respectively, while the bip ligand itself has an emission band at 411 nm (Supplementary material). The similarity of the emission bands of **1** and **2** to that of bip indicates that the luminescence for **1** and **2** may be intraligand fluorescent emission ($\pi$–$\pi^*$) [35]. The different emission positions and intensities of **1** and **2** may be attributed to the different structures. The enhancement of luminescence is associated with coordination of those ligands to the metal center, which effectively increased the asymmetry and rigidity of the ligands, thereby reducing the non-radiative decay of the intraligand excited state [36].

## 4. Conclusions

A number of zinc CPs of different network structures has been constructed by utilization of different carboxylates and N-heterocyclic ligands as building blocks [26–32]. Most unsymmetrical N-heterocyclic ligands coordinate to metal ions by chelating or monodentate modes [29–32]. Through assembly of rigid ligands $H_2$bpdc and $H_2$tdc with Zn(II) in the presence of unsymmetrical bip, we obtained two new CPs, $\{[Zn(bpdc)(bip)]\cdot 2H_2O\}_n$ (**1**) and [Zn(tdc)(bip)] (**2**), which are similar to those reported [32]. Consequently, change of the bridging ligand can influence the coordination environment of the metal and further influence the detailed architecture of the CPs as well as properties, such as the as-synthesized polymers **1** and **2,** exhibiting emission in the solid state at room temperature [32].

## Supplementary materials

Crystallographic data for the structural analysis have been deposited with the Cambridge Crystallographic Data Center, CCDC reference numbers: 905072 and 905073. These data can be obtained free of charge at http://www.ccdc.cam.ac.uk (or Cambridge Crystallographic Data Center, 12 Union Road, Cambridge CB2 1EZ, UK; Fax: +44-1223-336-033; E-mail: deposit@ccdc.cam.ac.uk).

## Acknowledgment

We thank the support of this work by NSFC (No. 31200642 and 41106146), Special Funds for the Basic R&D Program in the Central Non-profit Research Institutes (No. 20603022012018) and Special Scientific Research Funds for Central Non-profit Institutes, Chinese Academy of Fishery Sciences (No. 2013A1002).

## References

[1] O.K. Farha, O. Yazaydın, I. Eryazici, C. Malliakas, B. Hauser, M.G. Kanatzidis, S.T. Nguyen, R.Q. Snurr, J.T. Hupp. *Nat. Chem.*, **2**, 944 (2010).
[2] R. Poloni, B. Smit, J.B. Neaton. *J. Am. Chem. Soc.*, **134**, 6714 (2012).
[3] A. Shigematsu, T. Yamada, H. Kitagawa. *J. Am. Chem. Soc.*, **134**, 13145 (2012).
[4] J. An, C.M. Shade, D.A. Chengelis-Czegan, S. Petoud, N.L. Rosi. *J. Am. Chem. Soc.*, **133**, 1220 (2011).
[5] D. Buso, J. Jasieniak, M.D.H. Lay, P. Schiavuta, P. Scopece, J. Laird, H. Amenitsch, A.J. Hill, P. Falcaro. *Small*, **8**, 80 (2012).
[6] R.C. Huxford, J.D. Rocca, W. Lin. *Curr. Opin. Chem. Biol.*, **14**, 262 (2010).
[7] L.F. Ma, M.L. Han, J.H. Qin, L.Y. Wang, M. Inorg. *Chem.*, **51**, 9431 (2012).
[8] M.B. Lalonde, O.K. Farha, K.A. Scheidt, J.T. Hupp. *ACS Catal.*, **2**, 1550 (2012).
[9] P.Y. Wu, C. He, J. Wang, X.J. Peng, X.Z. Li, Y.L. An, C.Y. Duan. *J. Am. Chem. Soc.*, **134**, 14991 (2012).
[10] J.R. Li, J. Sculley, H.C. Zhou. *Chem. Rev.*, **112**, 869 (2012).
[11] G. Lu, J.T. Hupp. *J. Am. Chem. Soc.*, **132**, 7832 (2010).
[12] H.L. Jiang, D.W. Feng, T.F. Liu, J.R. Li, H.C. Zhou. *J. Am. Chem. Soc.*, **134**, 14690 (2012).
[13] S.S.Y. Chui, S.M.F. Lo, J.P.H. Charmant, A.G. Orpen, I.D. Williams. *Science*, **283**, 1148 (1999).
[14] C.J. Kepert, M.J. Rosseinsky. *Chem. Commun.*, **31**, (1998).
[15] B.L. Chen, M. Eddaoudi, S.T. Hyde, M. O'Keeffe, O.M. Yaghi. *Science*, **291**, 1021 (2001).
[16] H.K. Chae, D.Y. Siberio-Perez, J. Kim, Y. Go, M. Eddaoudi, A.J. Matzger, M. O'Keeffe, O.M. Yaghi. *Nature*, **427**, 523 (2004).
[17] T.F. Liu, J. Lu, R. Cao. *CrystEngComm*, **12**, 660 (2010).
[18] T.F. Liu, J. Lu, R. Cao. *Chem. Commun.*, **46**, 8439 (2010).

[19] P.P. Cui, J.L. Wu, X.L. Zhao, D. Sun, L.L. Zhang, J. Guo, D.F. Sun. *Cryst. Growth Des.*, **11**, 5182 (2011).

[20] X.L. Wang, B. Mu, H.Y. Lin, S. Yang, G.C. Liu, A.X. Tian, J.W. Zhang. *Dalton Trans.*, 11074 (2012).

[21] X.Q. Liang, D.P. Li, C.H. Li, X.H. Zhou, Y.Z. Li, J.L. Zuo, X.Z. You. *Cryst. Growth Des.*, **10**, 2596 (2010).

[22] J.Y. Lee, C.Y. Chen, H.M. Lee, E. Passaglia, F. Vizza, W. Oberhauser. *Cryst. Growth Des.*, **11**, 1230 (2011).

[23] G.Z. Liu, J.G. Wang, L.Y. Wang. *CrystEngComm*, **14**, 951 (2012).

[24] Y.L. Wang, J.H. Fu, Y.L. Jiang, Y. Fu, W.L. Xiong, Q.Y. Liu. *CrystEngComm*, **14**, 7245 (2012).

[25] A. Erxleben. *Coord. Chem. Rev.*, **246**, 203 (2003).

[26] Y.L. Chen, J. Yang, J.F. Ma. *J. Coord. Chem.*, **65**, 3708 (2012).

[27] H.L. Wen, T.T. Wang, C.B. Liu, M. He, Y.X. Wang. *J. Coord. Chem.*, **65**, 856 (2012).

[28] J.P. Zou, S.C. Dai, W.T. Guan, H.B. Yang, Y.F. Feng, X.B. Luo. *J. Coord. Chem.*, **65**, 2877 (2012).

[29] L.N. Yang, Y.X. Zhi, J.H. Hei, J. Li, F.X. Zhang, S.Y. Gao. *J. Coord. Chem.*, **64**, 2912 (2011).

[30] S.W. Jin, D.Q. Wang, Y.C. Xu. *J. Coord. Chem.*, **65**, 1953 (2012).

[31] C.Z. Li, X.R. Huang, Y.H. Chen. *J. Coord. Chem.*, **65**, 3699 (2012).

[32] D. Zhao, Y. Xiu, X.L. Zhou, X.R. Meng. *J. Coord. Chem.*, **65**, 112 (2012).

[33] Bruker AXS, *SAINT Software Reference Manual*, Madison, WI (1998).

[34] G.M. Sheldrick, *SHELXTL NT Version 5.1. Program for Solution and Refinement of Crystal Structures*, University of Göttingen, Germany (1997).

[35] X.L. Sun, Z.J. Wang, S.Q. Zang, W.C. Song, C. Cryst. *Growth Des.*, **12**, 4431 (2012).

[36] W. Chen, J.Y. Wang, C. Chen, Q. Yue, H.M. Yuan, J.S. Chen, S.N. Wang. *Inorg. Chem.*, **42**, 944 (2003).